2. M. Kronenberg, G. Siu, L. E. Hood, N. Shastri, *Annu. Rev. Immunol.* **4**, 529 (1986); J. P. Allison and L. L. Lanier, *ibid.* **5**, 503 (1987); B. Toyonaga and T. W. Mak, *ibid.*, p. 585; H. von Boehmer, *ibid.* **6**, 309 (1988).
3. P. Marrack and J. Kappler, *Science* **238**, 1073 (1987).
4. M. Blackman, J. Kappler, P. Marrack, *ibid.* **248**, 1335 (1990); H. von Boehmer and P. Kisielow, *ibid.*, p. 1369; F. Ramsdell and B. J. Fowlkes, *ibid.*, p. 1342.
5. D. G. Schatz, M. A. Oettinger, D. Baltimore, *Cell* **59**, 1035 (1989); M. A. Oettinger, D. G. Schatz, C. Gorka, D. Baltimore, *Science* **248**, 1517 (1990).
6. M. R. Lieber, J. E. Hesse, K. Mizuuchi, M. Gellert, *Genes Dev.* **1**, 751 (1987).
7. J. D. Ashwell and R. D. Klausner, *Annu. Rev. Immunol.* **8**, 139 (1990).
8. J. Sprent, in *Fundamental Immunology*, W. E. Paul, Ed. (Raven Press, New York, 1989), p. 69; R. G. Scollay, E. C. Butcher, I. L. Weissman, *Eur. J. Immunol.* **10**, 210 (1980); D. McGhee, J. Pye, K. Shortman, *Thymus* **1**, 151 (1979); B. J. Mathieson, and B. J. Fowlkes, *Immunol. Rev.* **82**, 141 (1984).
9. W. van Ewijk, P. L. van Soest, G. J. van den Engh, *J. Immunol.* **127**, 2594 (1981); K. Shortman, A. Wilson, W. van Ewijk, R. Scollay, *ibid.* **138**, 342 (1987); I. L. Weissman, *J. Exp. Med.* **137**, 504 (1973); R. Scollay and K. Shortman, *Thymus* **5**, 245 (1983); H. von Boehmer, *Annu. Rev. Immunol.* **6**, 309, 1988.
10. L. A. Turka *et al.*, unpublished observations.
11. C. A. Smith, G. T. Williams, R. Kingston, E. J. Jenkinson, J. J. T. Owen, *Nature* **337**, 181 (1989); D. J. McConkey, P. Hartzell, J. F. Amador-Perez, S. Orrenius, M. Jondal, *J. Immunol.* **143**, 1801 (1989); M. Mercep, A. M. Weissman, S. J. Frank, R. D. Klausner, J. D. Ashwell, *Science* **246**, 1162 (1989).
12. M. A. Nieto, A. Gonzalez, A. Lopez-Rivas, F. Diaz-Espada, F. J. Gambon, *J. Immunol.* **145**, 1364 (1990).
13. L. A. Turka *et al.*, *ibid.* **146**, 1428 (1991).
14. L. A. Turka *et al.*, unpublished observations.
15. L. E. Samuelson and R. D. Klausner, *Cell* **64**, 875 (1991).
16. J. P. Menetski and M. Gellert, *Proc. Natl. Acad. Sci. U.S.A.* **87**, 9324 (1990).
17. T. H. Finkel, P. Marrack, J. W. Kappler, R. T. Kubo, J. C. Cambier, *J. Immunol.* **142**, 3006 (1989); T. H. Finkel *et al.*, *Cell* **58**, 1047 (1989).
18. A. Winoto and D. Baltimore, *Cell* **59**, 649 (1989).
19. F. Triebel, R. Breathnach, M. Graziani, T. Hercend, P. Debre, *J. Immunol.* **140**, 300 (1988).
20. P. N. Marche and T. J. Kindt, *Proc. Natl. Acad. Sci. U.S.A.* **83**, 2190 (1986).
21. L. A. Matis, A. Ezquerra, J. E. Coligan, *J. Exp. Med.* **168**, 2379 (1988).
22. H. Von Boehmer, *Annu. Rev. Immunol.* **8**, 531 (1990).
23. In situ hybridization was performed as described [J. J. M. Chun *et al.*, *Cell* **64**, 189 (1991)] except that probes were labeled with digoxigenin and detected with an antibody to digoxigenin that was conjugated to alkaline phosphatase. Briefly, thymic sections (12 mm thick) were fixed and hybridized with RAG-1 or RAG-2 antisense or sense single-stranded RNA probes produced by in vitro transcription in the presence of digoxigenin-UTP. The RAG-2 antisense and sense probes consisted of nucleotides 1–1966 and 1–2062, respectively, of the RAG-2 cDNA [M. A. Oettinger *et al.*, in (*5*)]. The RAG-1 probe has been described [J. J. M. Chun *et al.*, *Cell* **64**, 189 (1991)]. In vitro transcription and detection of the probes were carried out with DIG RNA labeling kit and Genius Detection System (Boehringer Mannheim).
24. Thymic tissue was obtained from children under age 3 undergoing corrective cardiac surgery, and a single cell suspension of unseparated cells (Unsep) was prepared from tissue gently pressed through nylon mesh. Cells that were TCR-CD3$^-$ were isolated by negative selection with G19-4 (anti-CD3) and goat antibody to mouse immunoglobulin G (on coated magnetic beads) [L. A. Turka, J. A. Ledbetter, K. Lee, C. H. June, C. B. Thompson, *J. Immunol.* **144**, 1646 (1990)]. TCR-CD3$^+$ thymocytes were isolated by their adherence to tissue culture plates that were coated with a monoclonal antibody to CD3. Cells were allowed to adhere for 20 minutes, after which nonadherent cells were removed by vigorous washing. Mature single positive thymocytes were isolated by a two-step procedure. First, we negatively selected thymocytes with anti-CD8 MAb (G10.1 MAb) or with anti-CD4 MAb (G17-2) (gift of J. A. Ledbetter) on magnetic beads. The CD3$^+$CD4$^+$CD8$^-$ or CD3$^+$CD4$^-$CD8$^+$ cells were then purified by their adherence to anti-CD3–coated tissue culture plates and were >95% pure.
25. Northern blots were prepared from equalized samples of total cellular RNA. Each filter was hybridized with RAG-1, RAG-2, and HLA probes. The RAG-1 probe was a 0.9-kb Xho I-Hind III fragment corresponding to bases 2272 to 3180 [D. G. Schatz, M. A. Oettinger, D. Baltimore, *Cell* **59**, 1035 (1989)], and the HLA probe was a 1.4-kb Pst I fragment isolated from pHLA-B7 [A. K. Sood, D. Pereira, S. M. Weissman, *Proc. Natl. Acad. Sci. U.S.A.* **78**, 616 (1981)]. The RAG-2 probe was a 0.64-kb PCR product amplified from human genomic DNA with PCR primers corresponding to murine bases 825 to 845 and 1431 to 1459 in the sense and antisense strands, respectively [M. A. Oettinger, D. G. Schatz, C. Gorka, D. Baltimore, *Science* **248**, 1517 (1990)]. The sizes of the RAG-1 and RAG-2 mRNA species detected was comparable to those previously observed in pre-B and pre-T cell lines.
26. W. J. Leonard *et al.*, *Nature* **311**, 626 (1984).
27. P. Gunning *et al.*, *Mol. Cell. Biol.* **3**, 787 (1983).
28. We thank D. Baltimore, B. J. Fowlkes, D. Fox, J. Leiden, and B. Weber for reading of the manuscript. Supported by NIH grants DK-01899 (L.A.T.); Life and Health Insurance Medical Research Fund (D.G.S.); Whitaker Health Sciences Fund (M.A.O.); and the Helen Hay Whitney Foundation (J.J.M.C.).

19 February 1991; accepted 29 May 1991

Purification of an Allene Oxide Synthase and Identification of the Enzyme as a Cytochrome P-450

WEN-CHAO SONG AND ALAN R. BRASH*

Fatty acid hydroperoxides (lipoxygenase products) are metabolized to allene oxides by a type of dehydrase that has been detected in plants, corals, and starfish oocytes. The allene oxides are unstable epoxide precursors of more complex products such as jasmonic acid, the plant growth hormone. Characterization of the dehydrase enzyme of flaxseed revealed that it is a 55-kilodalton hemoprotein. The spectral characteristics of this dehydrase revealed it to be a cytochrome P-450. It operates with the remarkable activity of ≥1000 turnovers per second. The results establish a new catalytic activity for a cytochrome P-450 and illustrate the cooperation of different oxygenases in pathways of fatty acid metabolism.

ALLENE OXIDES ARE REACTIVE EPoxides that are prone to nucleophilic substitution and intramolecular rearrangements (*1*). The first allene oxides to be synthesized were small molecules designed with hydrophobic substituents to protect the epoxyene grouping from hydrolysis (*2*). Allene oxides have also been detected as natural products of lipid hydroperoxide metabolism (*3*). These allene epoxides are fleeting intermediates in the conversion of specific lipoxygenase products to more stable end products that include several prostaglandin-like molecules.

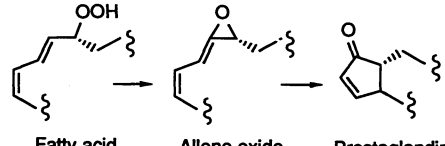

Biosynthesis of allene oxides involves an enzyme-catalyzed dehydration of the lipid hydroperoxide. The enzymes are selective for the position of the hydroperoxide group and the enantiomeric configuration (*3, 4*). We describe the purification of an allene oxide synthase (or hydroperoxide dehydrase) and its characterization as a member of the cytochrome P-450 family of hemoproteins.

As a source of enzyme, we used an acetone powder of flaxseed, a classic preparation of this type of hydroperoxide-metabolizing activity (*5*). Allene oxide synthase activity in fresh tissues is found in the microsomal fraction (*6*), but the acetone wash removes the microsomal lipids, and subsequent aqueous extraction of the acetone powder leaves the protein in a 100,000*g* supernatant. After initial ammonium sulfate fractionation of this extract, we examined the ability of the "redissolved" activity to pass through a standard 0.22-μm filter. Using this simple test in conjunction with a spectroscopic assay of enzyme activity, we established the efficiency of various detergents to effect complete solubilization. Use of 0.1 to 0.25% of the nonionic detergent Emulgen 911 (Kao-Atlas, Tokyo) not only allowed the free passage of the enzyme through the microfilters, it increased the

Department of Pharmacology, Vanderbilt University School of Medicine, Nashville, TN 37232.

*To whom correspondence should be addressed.

specific activity by two- to threefold. After solubilization, a scheme for chromatographic purification of the activity was developed (*7*). This resulted in approximately 500-fold purification of the enzyme (Table 1). In an SDS–polyacrylamide gel electrophoresis, the enzyme migrated with a molecular mass of 55 kD.

The cochromatography of this 55-kD protein with the enzyme activity was monitored carefully during the purification with anion exchange chromatography and chromatofocusing. The chromatofocusing step resolved two active isozymes with isoelectric points (pIs) of 5.5 and 5.4, respectively (Fig. 1). These two isozymes have indistinguishable electrophoretic mobilities, ultraviolet-visible (UV-Vis) spectra, and catalytic activities. Each purified isozyme was examined on a high-performance gel filtration column. The enzymic activity coeluted with the peak of UV absorbance, and the amount of activity closely paralleled the density of the 55-kD band found in individual fractions analyzed by SDS–polyacrylamide gel electrophoresis (Fig. 2).

The UV-Vis spectrum of the purified enzyme is shown in Fig. 3. This is the spectrum of a hemoprotein and is a perfect match for the spectrum of a cytochrome P-450 in the ferric, high-spin state (*8*). Diagnostic features include the location, shape, and relative absorbances of the Soret band at 392 nm, the broad band with angular shoulders at 512 nm and 540 nm, and the distinctive peak of absorbance at 643 nm (*8*). Reduction with dithionite led to the shift in the Soret band to 407 nm and other distinctive changes. The CO-binding spectrum of the reduced enzyme showed the expected absorbance maximum at 450 nm, the definitive property of a cytochrome P-450 (Fig. 3B). The 450-nm chromophore was fully developed within 2 min of adding dithionite; by 10 min it began to subside and was replaced with the characteristic chromophore of a cytochrome P-420. An unusual feature of the flaxseed enzyme is that the CO-Fe^{2+}–binding spectrum develops only to ~30% of the absorbance of the original 392-nm peak of the ferric enzyme (Fig. 3B). A high-spin oxidized form of cytochrome P-450 from tulip bulbs has similar spectral characteristics (*9*).

It is uncommon, though not unprecedented, to isolate a cytochrome P-450 in the high-spin pentacoordinated form (*10, 11*). Typically, the high-spin state is associated with the binding of substrate (*8*), which results in the displacement of water from the sixth ligand of the heme; the enzyme is then pentacoordinated. However, factors other than the substrate binding can produce the same effect. Single-mutation studies on mouse cytochrome P-450s suggest that the presence of a hydrophobic amino acid resi-

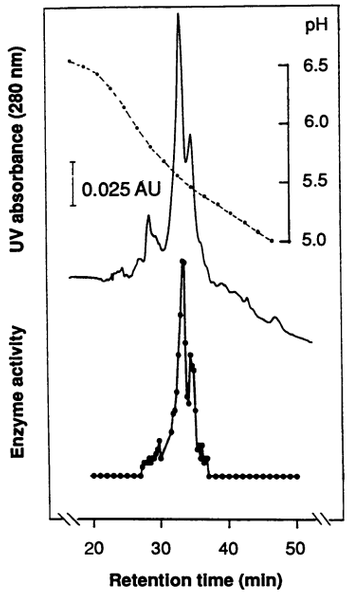

Fig. 1. Purification of flaxseed allene oxide synthase by chromatofocusing. The Mono-P HR 5/20 column (Pharmacia) was equilibrated with 25 mM bis-tris (pH 6.7) and 0.1% Emulgen 911. Sample was injected in 7 ml of the same buffer and then the column was eluted with 40 ml of Polybuffer 74 (Pharmacia), pH 5.0, and 0.1% Emulgen 911 at 1 ml/min. Aliquots of fractions were assayed for enzyme activity as described in Table 1. Enzyme activity eluted as two peaks at pIs 5.5 and 5.4.

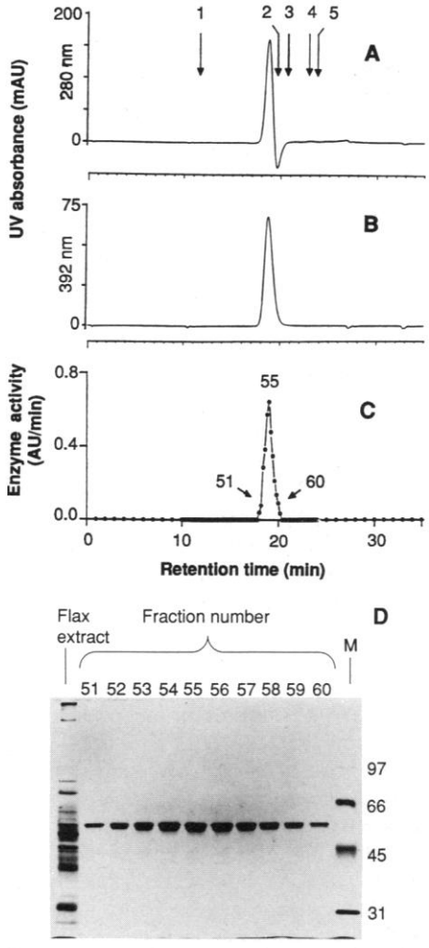

Fig. 2. High-performance gel filtration of purified allene oxide synthase; cochromatography of enzyme activity with the 55-kD protein. Enzyme (0.5 nmol) was chromatographed on a column of Superose 12 HR 10/30 (Pharmacia) in 50 mM phosphate buffer containing 0.1% Emulgen 911 at a flow rate of 0.7 ml/min. Fractions were collected every 1.0 or 0.2 min and assayed as described (Table 1). (**A**) Profile of the UV absorbance at 280 nm during the gel filtration experiment. Arrows indicate the position of molecular size markers: 1, Blue dextran (void volume); 2, albumin (67 kD); 3, ovalbumin (43 kD); 4, chymotrypsinogen A (25 kD) and 5, ribonuclease A (14 kD). (**B**) The corresponding profile at 392 nm; this wavelength is specific for the hemoprotein (Fig. 3). (**C**) The profile of enzyme activity. Numbers and dots indicate fraction numbers. (**D**) SDS–polyacrylamide gel electrophoresis of fractions collected across the peak of enzyme activity; proteins were detected by silver stain. M, molecular size markers (sizes shown at right in kilodaltons).

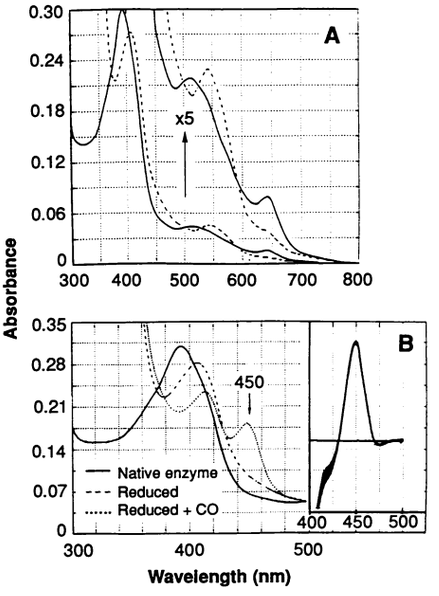

Fig. 3. UV-Vis absorption spectra of the purified allene oxide synthase. (**A**) The spectrum of the native enzyme (solid line) and the spectrum of the dithionite-reduced enzyme (dashed line) at pH 5.5 (in buffer from the Mono-P chromatography); the 450- to 800-nm regions are shown at fivefold higher sensitivity. (**B**) Comparison of the native enzyme with the dithionite-reduced enzyme before and after bubbling with CO. (Inset) Typical difference spectrum of the dithionite-reduced enzyme treated with CO. The two isozymes resolved on the Mono-P chromatofocusing column had indistinguishable UV-Vis spectral characteristics. Based on the quantitation of protein by amino acid analysis, the extinction coefficient of the native enzyme at 392 nm is 140 mM^{-1} cm^{-1}.

due close to the sixth ligand on the distal surface of the heme can prevent the binding of water and result in the high-spin electronic configuration (*12*).

We used the pure flaxseed enzyme to record the UV characteristics of the allene oxide in aqueous medium. The substrate 13-(*S*)-hydroperoxylinoleic acid was added to a cuvette containing sufficient enzyme to form the allene oxide product within 2 to 3 s. A series of spectra collected on a diode-array detector recorded the shift in UV absorbance that accompanies conversion to the allene oxide, which is followed by the rapid decomposition to more weakly absorbing ketols and cyclopentenone (Fig. 4A). From these recordings, we estimated the half-life of the allene oxide in this experiment to be ~9 s (at 10°C and pH 7) (Fig. 4B). High-performance liquid chromatography analysis of products from another experiment conducted with radiolabeled substrate showed the expected stable end products (Fig. 4, C and D). Based on UV measurements of the initial reaction rate at 25°C, the pure enzyme exhibits the remarkable catalytic activity of 70,000 to 80,000 turnovers per minute.

Table 1. Purification of flaxseed allene oxide synthase. Values are from an experiment starting with 20 g of acetone powder (7). From four enzyme preparations beginning with 5 to 40 g of acetone powder, the mean values (range in parentheses) of the final specific activities, recovery, and fold-purification were 17,300 AU mg^{-1} min^{-1} (14,660 to 21,740), 13.25% (11 to 16), and 512-fold (392 to 700), respectively. Enzyme activity was measured with a spectrophotometric assay (*5*). The substrate, 13-hydroperoxy linoleic acid (10 μg), was added in 5 μl of ethanol to 1 ml of 50 mM phosphate buffer and 10 mM octylglucoside (pH 7) in a 1-ml quartz cuvette. Reaction was initiated by addition of enzyme, and the initial rate of decrease in absorbance at 235 nm was measured as the substrate, 13-(*S*)hydroperoxylinoleic acid was converted to the allene oxide. The allene oxide in turn was instantly hydrolyzed, mainly to the non-UV absorbing α-ketol, 12-oxo-13-hydroxyoctadecenoic acid (*5*). Protein was determined with the Bio-Rad Protein Assay. As compared to the results of amino acid analysis, this colorimetric assay significantly overestimated the protein levels in the final steps of purification. AU, absorbance unit.

Purification step	Total protein (mg)	Specific activity (AU mg^{-1} min^{-1})	Recovery (%)	Purification (× fold)
Flax extract	3,398	32	100	
Ammonium sulfate (0–45%)	1,308	64	78	2
Octyl-Sepharose (CL-4B column)	50	989	46	31
Anion exchange (Mono-Q column)	4.2	9,990	39	315
Chromatofocusing (Mono-P column)	0.9	15,480	13	491

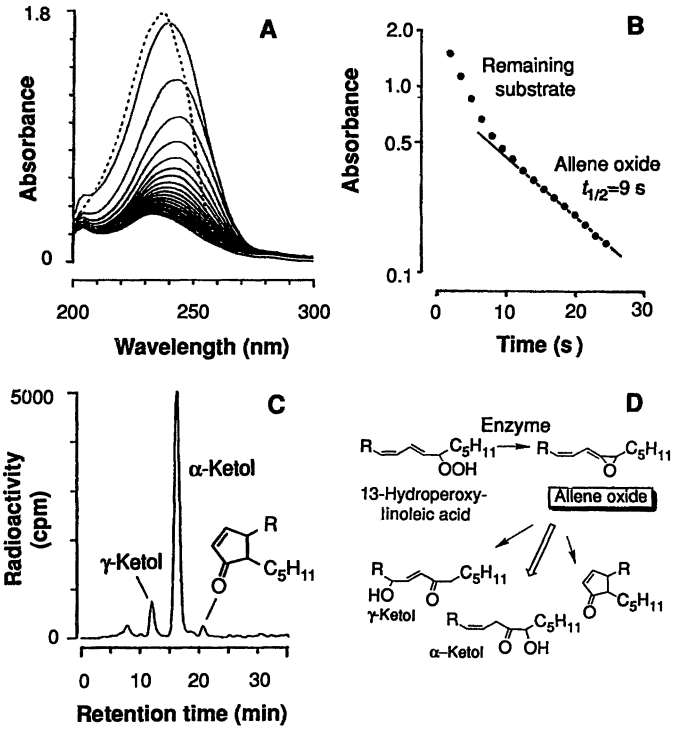

Fig. 4. Synthesis of allene oxide by the flaxseed hydroperoxide dehydrase and rapid allene oxide degradation by hydrolysis and cyclization. Enzyme (15 pmol) was equilibrated at 10°C in 1 ml of 50 mM phosphate buffer and 10 mM octylglucoside (pH 7) in the quartz glass cuvette of a diode-array spectrophotometer (Hewlett-Packard). Reaction was initiated by the addition and rapid mixing of an ethanolic solution of the 13-(*S*)-hydroperoxide of linoleic acid (final concentration 90 μM, 2.05 AU at 235 nm). After 2 s, a series of UV spectra were acquired at 1.5-s intervals. (**A**) Overlay of the UV spectra. The dotted line is the spectrum of pure substrate recorded in the absence of enzyme. (**B**) Semilogarithmic plot of the UV absorbance versus the time after addition of substrate. (**C**) Reversed-phase high-performance liquid chromatography analysis of the stable end products of allene oxide degradation from a separate incubation with radiolabeled substrate. Column, Beckman 5-μm ODS Ultrasphere (25 cm by 0.46 cm); solvent, acetonitrile–water–acetic acid, 60:40:0.01 by volume; flow rate, 1 ml/min. (**D**) Scheme of allene oxide synthesis and degradation.

The allene oxide synthase activity is unique among the known reactions catalyzed by cytochrome P-450 enzymes. Nevertheless, the dehydrase reaction of the allene oxide synthase can be rationalized in terms of the known chemistry of cytochrome P-450–catalyzed reactions. For example, the dehydrase reaction can be viewed as a two-step process: homolytic cleavage of the hydroperoxide and hydrogen abstraction from the β carbon, followed by formation of a carbon-oxygen bond. This type of scheme is in agreement with current concepts of the catalytic mechanisms of cytochrome P-450 reactions (*13*).

Characterization of the flaxseed allene oxide synthase as a cytochrome P-450 identifies an unusual example of direct cooperation of different oxygenases in a biosynthetic pathway. In the principal sequence of reactions, linolenic acid is oxygenated by a lipoxygenase, the resulting 13-hydroperoxide is converted to an allene oxide by the cytochrome P-450, and finally the allene oxide is the substrate of an allene oxide cyclase, giving a direct analog and metabolic precursor of jasmonic acid, the plant growth regulator (*14*). Allene oxides also are formed in the animal kingdom; they have been detected in several species of marine invertebrates (*15, 16*). In the examples detected so far, the allene oxide synthases in animals are specific for the 8-(*R*)-hydroperoxide of arachidonic acid; the plant 13-hydroperoxides are not substrates (and vice versa). There are strong parallels between the animal and plant systems, and it appears likely that these allene oxide synthases may be a class of related cytochrome P-450s.

REFERENCES AND NOTES

1. T. H. Chan and B. S. Ong, *J. Org. Chem.* **43**, 2994 (1978); *Tetrahedron* **36**, 2269 (1980).
2. R. L. Camp and F. D. Greene, *J. Am. Chem. Soc.* **90**, 7349 (1968); J. K. Crandall and W. H. Machleder, *J. Heterocycl. Chem.* **6**, 777 (1968).
3. E. J. Corey, M. d'Alarcao, S. P. Matsuda, P. T. Lansbury, Jr., *J. Am. Chem. Soc.* **109**, 289 (1987); M. Hamberg, *Biochim. Biophys. Acta* **920**, 76 (1987); A. R. Brash, S. W. Baertschi, C. D. Ingram, T. M. Harris, *J. Biol. Chem.* **262**, 15829 (1987); L. Crombie and D. O. Morgan, *J. Chem. Soc. Chem. Commun.* **1988**, 558 (1988).

4. S. W. Baertschi, C. D. Ingram, T. M. Harris, A. R. Brash, *Biochemistry* **27**, 18 (1988).
5. D. C. Zimmerman, *Biochem. Biophys. Res. Commun.* **23**, 398 (1966); B. A. Vick and D. C. Zimmerman, *Plant Physiol.* **46**, 445 (1970); D. C. Zimmerman and P. Feng, *Lipids* **13**, 313 (1977).
6. B. A. Vick and D. C. Zimmerman, *Plant Physiol.* **67**, 92 (1981); S. Grossman, I. Shanin, B. Sredni, *Biochim. Biophys. Acta* **572**, 65 (1983); B. A. Vick and D. C. Zimmerman, *Plant Physiol.* **85**, 1073 (1987); M. Hamberg, *Biochim. Biophys. Res. Commun.* **156**, 543 (1988).
7. Flaxseed acetone powder (20 g, 50 mg/ml) was extracted at 0°C with 50 mM phosphate buffer, pH 7.0 (buffer A) (*5*). The 10,000*g* supernatant was fractionated with ammonium sulfate (0 to 45% at 0°C). The precipitate was applied to a column of octyl-Sepharose CL-4B (Pharmacia, 50-ml bed volume) in 95 ml of buffer A with 0.5 M ammonium sulfate and 0.25% (w/v) Emulgen 911. After extensive washing with buffer A containing 0.5 M ammonium sulfate, we eluted the activity with buffer A containing 0.25% Emulgen 911. The active fractions were then applied to a Mono-Q HR 5/10 column (Pharmacia) in 20 mM triethanolamine (pH 7.3) and 0.1% Emulgen 911 (buffer B). The column was eluted at 1 ml/min with a gradient of buffer B containing 0.5 M NaCl (buffer C); activity eluted at 20% buffer C. Finally, the enzyme was purified on a Mono-P HR 5/20 chromatofocusing column (Pharmacia) (Fig. 1). Centriprep-30 concentrators (Amicon) were used for concentrating enzyme fractions and PD-10 columns (Pharmacia) were used for buffer exchange. Chromatography was carried out at room temperature; at all other times the enzyme was kept at 0°C.
8. C. R. E. Jefcoate and J. L. Gaylor, *Biochemistry* **8**, 3464 (1969); J. A. Peterson, *Arch. Biochem. Biophys.* **144**, 678 (1971); D. A. Haugen and M. J. Coon, *J. Biol. Chem.* **251**, 7929 (1976).
9. K. Higashi *et al.*, *Agric. Biol. Chem.* **49**, 2399 (1985).
10. S. D. Black and M. J. Coon, in *Cytochrome P-450: Structure, Mechanism, and Biochemistry*, P. R. Ortiz de Montellano, Ed. (Plenum, New York, 1986), chap. 6.
11. The term "high-spin" refers to the distribution of the *3d* electrons of the heme iron; high-spin is synonomous with a low-energy field surrounding the iron. This permits the distribution of electrons into the higher-energy orbitals, giving the high-spin state.
12. M. Iwasaki, R. Juvonen, R. Lindberg, M. Negishi, *J. Biol. Chem.* **266**, 3380 (1991).
13. F. P. Guengerich, *Crit. Rev. Biochem. Mol. Biol.* **25**, 97 (1990).
14. B. A. Vick and D. C. Zimmerman, *Biochem. Biophys. Res. Commun.* **111**, 470 (1983); M. Hamberg and P. Fahlstadius, *Arch. Biochem. Biophys.* **276**, 518 (1990).
15. E. J. Corey, S. P. T. Matsuda, R. Nagata, M. B. Cleaver, *Tetrahedron Lett.* **29**, 2555 (1988); A. R. Brash, *J. Am. Chem. Soc.* **111**, 1891 (1989).
16. An allene oxide synthase activity is present in starfish oocytes; the cells convert 8-(*R*)-hydroperoxyeicosatetraenoic acid to the allene oxide 8,9-epoxyeicosatetra-5,9,11,14-enoic acid (A. R. Brash, M. A. Hughes, D. J. Hawkins, W.-C. Song, unpublished observations).
17. We thank W. E. Boeglin for technical assistance, T. J. Lucas for amino acid analysis, and F. P. Guengerich for helpful discussions and for a critical reading of the manuscript. Supported by NIH grant number DK-35275.

27 March 1991; accepted 5 June 1991

Specificity for Aminoacylation of an RNA Helix: An Unpaired, Exocyclic Amino Group in the Minor Groove

KARIN MUSIER-FORSYTH, NASSIM USMAN, STEPHEN SCARINGE, JENNIFER DOUDNA, RACHEL GREEN, PAUL SCHIMMEL*

An acceptor stem G3·U70 base pair is a major determinant of the identity of an alanine transfer RNA. Hairpin helices and RNA duplexes consisting of complementary single strands are aminoacylated with alanine if they contain G3·U70. Chemical synthesis of RNA duplexes enabled the introduction of base analogs that tested the role of specific functional groups in the major and minor grooves of the RNA helix. The results of these experiments indicate that an unpaired guanine 2-amino group at a specific position in the minor groove of an RNA helix marks a molecule for aminoacylation with alanine.

CONTACTS OF PROTEINS BOUND TO the B-form DNA helix are commonly made through base-specific hydrogen bond donor and acceptor groups that lie in the major groove, which is sufficiently wide to accommodate an α helix or other structural motifs. The groups in the major groove include guanine and adenine N-7, guanine O-6, adenine 6-amino, thymine O-4, and cytosine 4-amino. Amino acid side chains and the peptide backbone provide complementary hydrogen-bonding groups on proteins that enable all base pairs in DNA to be distinguished, in principle, on the basis of major-groove interactions (*1*). In contrast, RNA helices are A-form structures that have deep but narrow major grooves that limit accessibility of protein side chains on α helices or other motifs. Although there are fewer hydrogen-bonding possibilities in the minor groove to allow discrimination among the base pairs in duplex RNA, the minor groove of the A form is wide and shallow and is readily accessible to side chains that emanate from structural elements of proteins (*1, 2*).

These considerations have relevance to the molecular basis for the discrimination of tRNAs by aminoacyl tRNA synthetases. These discriminations provide the basis for the genetic code whereby amino acids are assigned to nucleotide triplets (anticodons) that are encoded by tRNAs. For Ala and His tRNAs, the anticodon and other parts of the tRNA are dispensable for aminoacylation (*3*). Small RNA hairpin helices that reconstruct the acceptor end of these tRNAs can be aminoacylated with complete specificity. In the case of Ala, aminoacylation requires a single G3·U70 base pair in both prokaryotic and eukaryotic Ala tRNAs (*4*). Alteration of this base pair to G·C, A·U, or U·G abolishes in vitro aminoacylation with Ala (*5*).

RNA duplexes composed of complementary single strands are also aminoacylated with Ala, provided that they contain G3·U70 (*6*). The complementary single strands can easily be synthesized by chemical methods that use fully protected diisopropylamino-β-cyanoethyl ribonucleoside phosphoramidites (*7*). These methods provide the opportunity to synthesize protected ribonucleoside phosphoramidites of two-base analogs that, when introduced in place of G3·U70, can be used to identify the atomic group (or groups) at the 3·70 position that are essential for aminoacylation.

The G4·U69 base pair is in the wobble configuration in the three-dimensional structure of yeast $tRNA^{Phe}$ (*8*), and nuclear magnetic resonance experiments have established the wobble pairing for the G3·U70 base pair in an Ala minihelix (*9*). The N-7 and O-6 atoms of G3 and O-4 of U70 project into the major groove, whereas N-3, the 2-amino group of G3, and O-2 of U70 lie in the minor groove of the A-form RNA helix (Fig. 1). Inosine (I), which lacks an exocyclic 2-amino group, forms the same wobble-like pair with uracil as guanine does (Fig. 1). Except for the 2-amino group of G3, the I3·U70 base pair retains all major and minor groove base atoms in the same orientation as G3·U70.

The fully protected inosine phosphoramidite was synthesized using the same protecting group strategy used for the standard ribonucleosides A, C, G, and U (*7*). This method involves the use of the *tert*-butyldimethylsilyl protecting group for the 2′-hydroxyl and a 3′-β-cyanoethyl *N,N*-diisopropylamino phosphoramidite group for formation of the internucleotide linkage (*10*). Inosine was introduced by solid-phase chemistry separately into positions 3 and 4 of a duplex that is based on the sequence of the first nine base pairs of the acceptor TΨC stem of *Escherichia coli* $tRNA^{Ala/GGC}$ (Fig. 2). These molecules are designated I3·U70/

K. Musier-Forsyth, N. Usman, P. Schimmel, Department of Biology, Massachusetts Institute of Technology, Cambridge, MA 02139.
S. Scaringe, Department of Chemistry and Biochemistry, University of Colorado, Boulder, CO 80309.
J. Doudna and R. Green, Department of Molecular Biology, Massachusetts General Hospital, Boston, MA 02114.

*To whom correspondence should be addressed.